Available online at www.sciencedirect.com

SciVerse ScienceDirect

Procedia Environmental Sciences 19 (2013) 885 – 894

Procedia Environmental Sciences

Four Decades of Progress in Monitoring and Modeling of Processes in the Soil-Plant-Atmosphere System: Applications and Challenges

Hyperspectral image analysis in environmental monitoring: setup of a new tunable filter platform

Monica Moroni[a]*, Emanuela Lupo[a], Emanuela Marra[a], Antonio Cenedese[a]

DICEA-Sapienza University of Rome, via Eudossiana 18, 00184 Rome, Italy

Abstract

Nowadays, acquisition and analysis of hyperspectral images represent a new frontier among environmental monitoring techniques. Tunable filters and spectrometers, coupled to appropriate sensors, can be used to acquire the spectral information of large areas (more than 10 km^2) with great accuracy. The analysis of hyperspectral images provides the spatial distribution (maps) of terrain physical and ecological characteristics. The maps are created by processing the fraction of the incident solar radiation reflected by each object located on the terrain as a function of the wavelength. This feature is known as to "spectral signature". The aim of the research conducted at DICEA - Sapienza University of Rome is to test the applicability and potentiality of these novel instrumentations to applications in natural and artificial systems. In particular, the environmental status of the region crossed by the Sacco river (Latium, Italy) was investigated by analyzing the spectral response given by tree samples located upstream and downstream an industrial area interested by assessed contamination episodes. Data acquired were synthesized in two reflectance indices related to the chlorophyll content: the normalized difference vegetation index and a modified version. The acquisition campaigns described here have helped the set-up and improvement of the hyperspectral image system based on the use of tunable interference filters. Reflectance values and indices suggest tree samples located upstream the contaminated area are 'healthier' than those downstream.

Keywords: hyperspectral imaging, monitoring, proximal sensing, contamination

1. Introduction

Hyperspectral remote and proximal sensing is currently extensively and successfully used to study the

* Corresponding author. Tel.: +390644585638; fax: +390644585094.
E-mail address: monica.moroni@uniroma1.it.

doi:10.1016/j.proenv.2013.06.098

state of the environment and to track changes that occur over time.

Hyperspectral images of objects placed some hundreds of meters apart are generally acquired with equipment mounted on fixed stands (usually located uphill) or with airborne platforms.

Generally, spectra are evaluated in three wavelength ranges:

- visible (VIS) from 300 nm to 750 nm;
- near infrared (SNIR) from 700 nm to 1000 nm;
- mid infrared (LNIR) from 900 nm to 2000 nm;

In these ranges, the energy due to the reflection of solar radiation is several orders of magnitude larger than the energy emitted due to the body temperature which is therefore negligible.

The spectral signature describes the fraction of incident solar radiation reflected from the surface of the object as a function of wavelength. Each object presents a typical reflectance spectrum that can be used to distinguish it from other objects. The variation of the reflectivity of an object is generally large and depends on the characteristics of the materials but also on lighting conditions, environmental conditions and characteristics of the instrumentation used.

In practice, during the data acquisition stage, the light reflected from the objects is discretized into n components within the electromagnetic spectrum. The number of bands determines the type of sensor, multispectral rather than hyperspectral. Multispectral sensors evaluate few wavelengths (maximum 10) whereas for hyperspectral sensors a number of wavelengths greater than 10 is evaluated.

The starting dataset for hyperspectral analysis is the hyperspectral cube, constructed by superimposing n images, namely cube bands, each representing the same spatial coordinates (the same piece of land) but different radiometric information.

The applications of hyperspectral imaging to natural resources, vegetation and surface water, have been widely tested. The spectral signature of vegetation is influenced by the presence of pigments (mainly chlorophyll-a, chlorophyll-b, xanthophyll and carotenoids), whose content varies depending on the chemical and biological activity of the plant [1-3], the physical structure and water content of leaves [4]. The reflectance spectrum of a plant provides information on the degree of senescence, the deterioration of leaf structure or any diseases and abnormalities the plant may be affected from [4, 1, 5]. Gamon and Surfus (1999) [6] reported quantitative estimates of chemical content in leaves and canopies using indices derived from spectral reflectance at specific wavelengths. Because of the links between chemical content and leaf structure and function, a number of important ecophysiological properties can be inferred from these reflectance indices. Thenkabail et al. (2002) [7] determined the optimal hyperspectral narrow wavebands, in the visible and near-infrared portion of the spectrum, that best characterize agricultural crop characteristics. Vegetation indices derived from narrow and broad wavebands were used to establish relationships with crop biophysical variables and yield. Hyperspectral analysis of surface water bodies (lakes, rivers and coastal waters with riparian zones) provides information on key water quality parameters (chlorophyll-a, suspended solid content, turbidity, etc..) and its trophic state [8]. In fact, the reflectance of the water surface is the result of complex processes of absorption and reflection of sunlight by phytoplankton, inorganic particles in suspension, dissolved humus, water plants and water. Studies carried out by satellite sensors have demonstrated the relationship between surface reflectance, turbidity and chlorophyll-a content. The content of chlorophyll-a is proportional to the amount of biomass present in the body, while there is a relationship between reflectance and total suspended solids [9]. Another application of hyperspectral analysis for the study of surface water bodies is the monitoring of the morphology of the lagoon area and distribution of halophilic vegetation in intertidal environments, due to the high temporal resolution airborne sensors [10].

At the Laboratory of Hydraulics of DICEA-Sapienza University of Rome, an effective methodology for hyperspectral monitoring has been developed. It is based on the use of two innovative experimental devices for acquiring hyperspectral images, one based on the use of tunable interference filters, the other

on the use of spectrometers. Both systems allow sampling the spectral range 400-1800 nm. The system with interference filters has been employed for recognition of vegetation, and detecting diseases and abnormalities in the spectral signatures of plant species [11]. The system with spectrometers and an original algorithm for automatically combining multiple, overlapping images of a scene to form a single composition, have been employed in a proximal sensing field campaign conducted in San Teodoro (Olbia-Tempio—Sardinia). Mapping allowed for the identification of objects within the acquired image and agreed well with ground-truth measurements [12].

The systems developed have very unique and qualifying characteristics:

- low cost if compared to other system available on the market;
- high spectral resolution;
- high spatial and temporal resolution;
- easy portability, both systems have been engineered so that they can be transported by ultralight airplanes.

In this paper we present the data acquired during a proximal sensing field survey conducted in the valley of the Sacco river (Latium, Italy) with the tunable interference filter platform. This study is part of a larger project dedicated to the recovery and requalification of that area, subject in the last few years of a number of alarming cases of pollution. The hyperspectral analysis was employed to detect the environmental status of the region crossed by the river. This was achieved by analyzing the spectral response given by tree samples located upstream and downstream an industrial area interested by assessed contamination episodes.

To express pigment content and infer modification of the plant ecophysiological state, eventually related to the contamination of the area, we calculated reflectance indices, which are mathematical expression derived from reflectance spectra. These indices allow capturing essential features of the spectra and reducing a large volume of data to a single, workable value to facilitate plotting and statistical analyses. Two indices were used in this study: (1) the normalized difference vegetation index (NDVI); and (2) a modified version of the NDVI ($NDVI_{705}$). Both are indices of the chlorophyll content, (3) is an index of anthocyanin content. It is worth noting NDVI has been widely used since the 1970s whereas $NDVI_{705}$ was introduced later as an improvement considering a narrow waveband at the edge of the chlorophyll absorption feature (e.g. 705 nm) rather than at the middle [6].

2. System based on tunable filters

The system is based on the use of three Varispec tunable filters (Figure 1). Each filter is mounted in front of the sensor lens. The wavelength of transmitted light is electronically controllable through liquid crystal elements. The first filter frequencies range between 400 nm and 720 nm (VIS filter), the second one between 650 nm and 1100 nm (SNIR filter); the third one between 850 nm and 1800 nm (LNIR filter). Images at a given wavelength (the bandwidth is 10 nm) are then obtained. It is necessary to acquire more pictures to gather the full spectrum of the scene.

Figure 2 shows the diagram of the system configuration, comprising:

- one high-speed DVR (frame grabber) with three Camera Link inputs (IO Industries DVR Express® Blade) to acquire and manage the data from the cameras and with a trigger signal generator to tune the filter frequency;
- one 1-terabyte solid state disk array;
- one VIS filter (F1) mounted in front of a Dalsa 4M60 CMOS camera (2,352 × 1,728 pixels @ 25 fps);
- one SNIR filter (F2) mounted in front of a Dalsa 4M60 CMOS camera (2,352 × 1,728 pixels @ 25 fps);
- one LNIR filter (F3) mounted in front of a Xeva Xenics InGaAS camera (640 × 512 pixels @ 25 fps);

- one thermal camera;
- one power supply system for all devices;
- one processing computer for controlling the entire system and acquiring images of the thermal camera via a USB port (the thermal images are not discussed in this contribution).

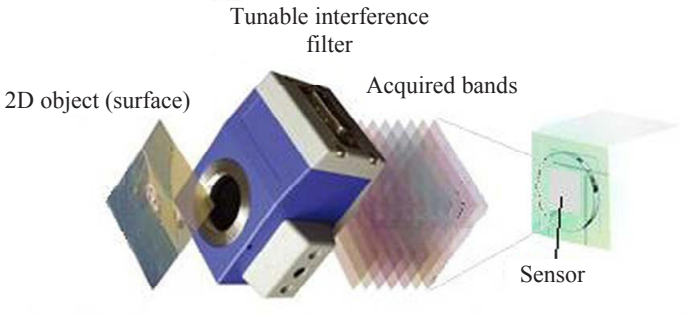

Figure 1. Sketch of a tunable interference filter

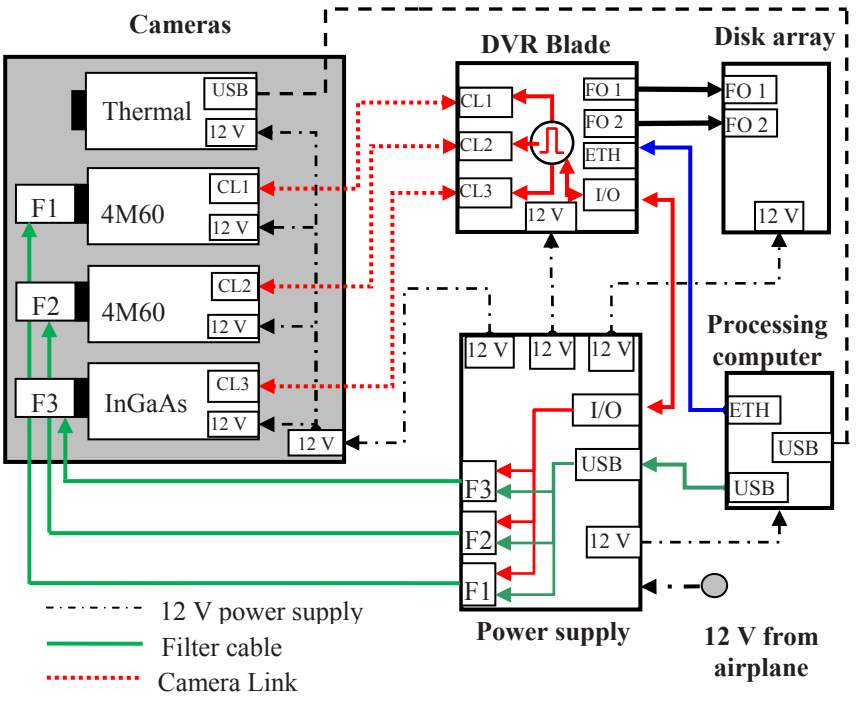

Figure 2. Apparatus with interferential filters

3. Analysis of hyperspectral images

The acquired images are analyzed by specifically developed software and by commercial software (ENVI).

The main steps of the analysis are listed below.

Elimination of vignetting effects on each image. This imperfection causes the reduction of brightness at image edges respect to its center. It is due to the camera lens and to the tunable filters placed in front of the camera.

Noise filtering. The CMOS and InGaAs arrays employed for image acquisitions are subject to various sources of noise, including thermal noise, shot noise, and electronic noise in the amplified circuitry. When the image is digitized, it also suffers intensity quantization, usually to 8 bits of resolution.

Construction of the hyperspectral cube. Since data have been acquired from three cameras, a geometric transformation (warping) was required to place all the images on a same reference system.

Radiometric calibration. It constitutes one of the most sensitive pre-processing steps, since it ensures the construction of a spectral library as close as possible to the material characteristics. This is achieved by eliminating the dependence on the spectra of the measuring instruments (quantum efficiency of the sensor, filter transmission). In fact, the acquisition system does not record the material reflectance but rather the value of radiance, or that part of the reflected radiation that reaches the camera sensor with an energy content sufficient to be recorded. The absolute reflectance of the materials can be calculated only if the incident radiation on the target is known. In this case, being the source of radiation the Sun, it would be impossible to obtain the value of radiation incident on each point of the scene. The relative reflectance is then calculated. This is achieved by comparison with a reference spectrum chosen ad hoc. Two methods can be employed: the Internal Average Relative Reflectance and the Flat Field. The first method derives correction parameters directly from the images while the second one requires the presence of targets with smooth reference reflectance spectrum.

Clustering and extraction of spectral signatures. This step is performed on the radiometrically calibrated hyperspectral cube to produce a thematic map of the site under study, i.e., an image in which pixels with similar spectral signature are associated to the same class. The spectral classification process requires the definition of a spectral library, the implementation of an algorithm for image mapping, management of information extracted. Classification algorithms can be supervised or unsupervised. Supervised classification is comprised of two steps. The image analyst "supervises" the pixel categorization process by specifying various land cover types present in the scene. To perform this supervision, representative sample sites of known cover type, known as training areas, are used to describe the spectral attributes for each feature type of interest. Next, each pixel in the data set is numerically compared to each category that is identified and labeled with the name of the category with the greatest similarity [13]. Alternatively, in the non-supervised classification algorithm, the labeling is done by comparing reflectance spectra of all image pixels. At the end of the classification process, the cumbersome set of hyperspectral data is synthesized into a thematic map that categorizes different materials and different conditions on the ground.

Calculation of reflectance indices. Assuming R refers to reflectance, the subscripts refer to specific spectral bands or wavelengths (i.e., NIR refers to the average in the band interval 750-1100 nm, VIS to the average in the band interval 580-750 nm; 750 and 705 refer to narrow wavelengths at 750 nm and 705 nm respectively), reflectance indices may be calculated as follows:

$$\mathrm{NDVI} = \frac{R_{\mathrm{NIR}} - R_{\mathrm{VIS}}}{R_{\mathrm{NIR}} + R_{\mathrm{VIS}}} \quad (1)$$

$$\mathrm{NDVI}_{705} = \frac{R_{750} - R_{705}}{R_{750} + R_{705}} \quad (2)$$

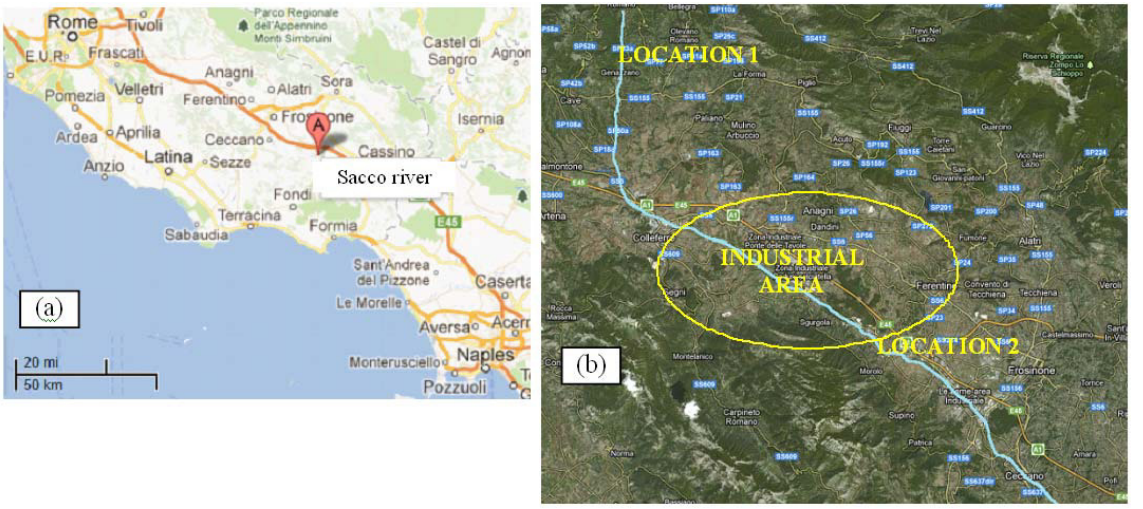

Figure 3. (a) Map for localizing the area of study; (b) Zoom in the area of study and location of measuring stations

4. Characterization of the study area

The Sacco river, sub basin of river Liri-Garigliano, arises from Monte Casale, belonging to the complex of Monti Prenestini. Its waters cross the Province of Frosinone, near the town of Paliano, then flowing in the Province of Rome in the municipalities of Genazzano, Valmontone and the city of Colleferro, returning in the province of Frosinone. The river continues toward the Latin valley, collecting waters of the tributaries from the Ernici and Lepini mountains and finally pouring its waters into the river Liri at Ceprano (Figure 3a).

The Sacco river valley hosts numerous municipalities and is characterized by the presence of several industrial facilities (chemical, mechanical, electronic and food) and intense farming activities. One of the main issues for the environmental remediation of this territory concerns the proven presence in soil and irrigation water of β-hexachlorocyclohexane ($C_6H_6Cl_6$), stable isomer of lindane, used as a pesticide until its prohibition.

Data were collected in five proximal sensing surveys, which took place in 2010, 2011 and 2012. The information concerning the measurement campaigns are reported in Table 1. In particular, the table reports the object employed for the radiometric calibration of the hyperspectral data.

Table 1. Dates of the Sacco river field survey.

Field survey	Date	location		Calibration object
1	October 1st, 2010	1	-	Polystyrene
2	October 29th , 2010	1	2	Polystyrene
3	July 30, 2011	-	2	Spectralon
4	October 11st, 2011	1	2	Spectralon
5	June 25th, 2012	1	2	Spectralon

The field survey interested two sections of the river: one (location 1), in the municipality of San Vito, is located upstream the area that is supposed to be contaminated, the other (location 2), in Ponte of Tomacella (Patrica), is located downstream (Figure 3b). Both areas are characterized by a certain vegetation homogeneity with the predominant presence of White Willow (*Salix Alba*) and, to a lesser extent, of Black Poplar (*Populus Nigra*). The acquisition system was placed in both locations on the ground. The images were acquired as the sun was roughly at its zenith, in particular between 10 a.m. and 3 p.m., in order to provide the maximum sunlight. The scene was orthogonal to the optics and at a distance of a few tens of meters. Figure 4a shows an image of the Salix monitored in location 1, Figure 4b is relative to the Salix of location 2.

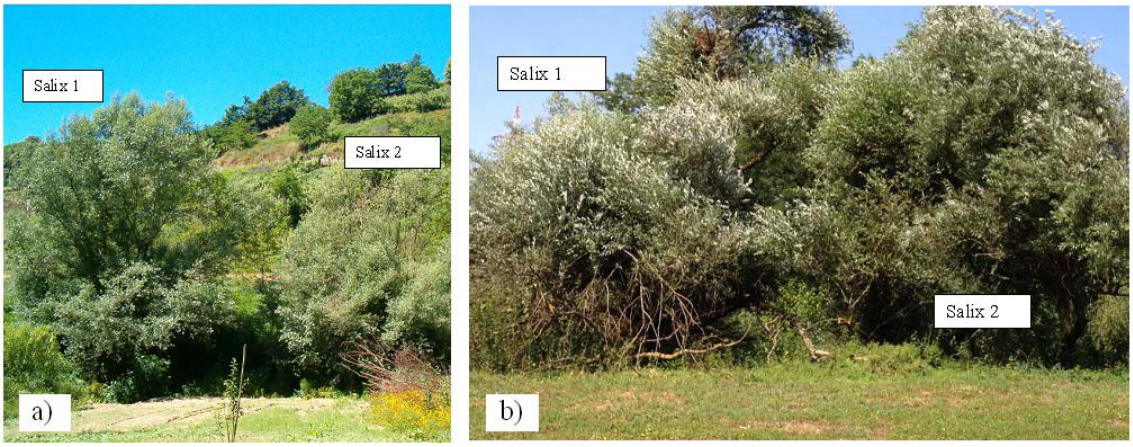

Figure 4. Salix monitored in location a) 1 and b) 2

5. Results

In this contribution we will present the results of the field survey #5. For the complete set of results refer to [14].

Vignetting effects were modeled by a $\cos^4(\alpha)$ fall-off in intensity away from the principal point, assuming that the optic axis passes through the image center. To reduce noise effects, images have been convolved with a Gaussian mask. No appreciable effects, such as blur, have been noticed in the resulting images. Bad pixels in the images acquired with the Xeva Xenics InGaAS camera have been removed prior to the Gaussian filter was applied.

In Figure 5, the hyperspectral cube of Salix 2 in location 2 (built with 141 images ranging from wavelengths of 400 nm to 1,800 nm with a step of 10 nm) is displayed in RGB using images at the 620 nm (R), 560 nm (G) and 480 nm (B) bands.

For the radiometric calibration of the hyperspectral cubes, the Flat Field method was employed by introducing in the scene a white reference standard (Spectralon target).

Tree samples at location 1 and 2 exhibit characteristic patterns of spectral reflectance in the range 400-1800 nm, as illustrated in Figure 6.

Both spectral signatures reflect the typical behavior of vegetation presenting two chlorophyll wells at the wavelengths of blue and red, a green peak, which is not very clear although present, corresponding to the wavelength of green, the red edge and NIR plateau. In the region of LNIR (1100-1800 nm) the

spectral response of vegetation is affected by atmospheric water molecule filtering of part of the solar radiation incident on our planet which creates windows of absorption around 1100 nm and 1400 nm.

Figure 5. Hyperspectral cube of Salix 2 in location 2 displayed in RGB using images at bands 620 nm (R), 560 nm (G) and 480 nm (B).

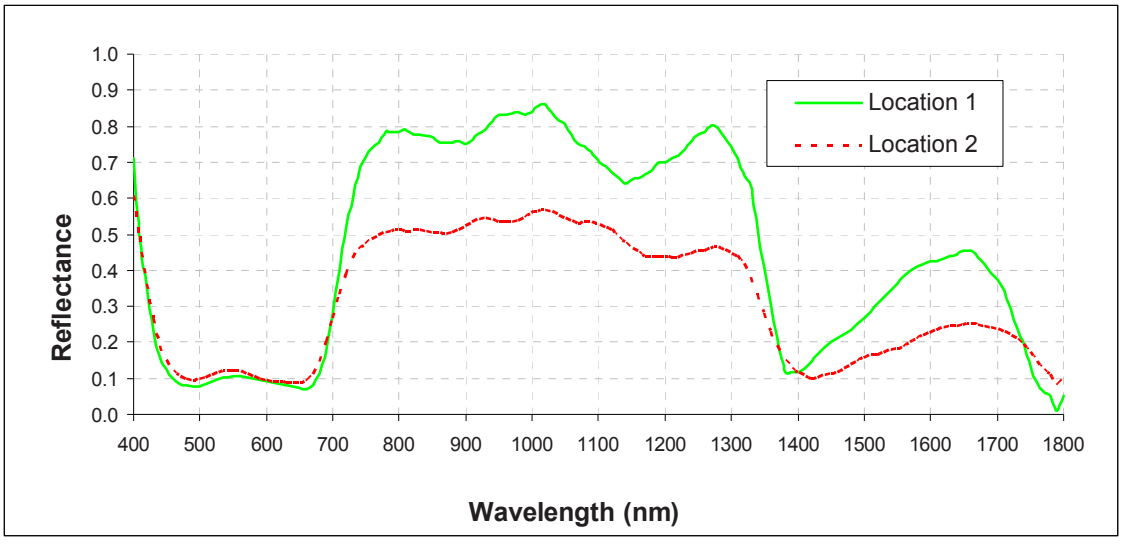

Figure 6. Representative reflectance spectra of Salix samples of location 1 (green-solid line) and 2 (red-dashed line)

The comparison between the curves in the visible region does not illustrate substantial differences in terms of reflectance values and wavelengths corresponding to the feature investigated. In the near infrared

region, from wavelength 700 nm, a significant reduction of reflectance occurs, for all wavelengths detected, for Salix 1 of the location 2. In the NIR region, the value for reflectance is related to the water content within the leaf, which, in condition of stress, undergoes an alteration in terms of internal distribution with a consequent significant variation for the spectral response.

The tree samples investigated in the location 1 exhibit higher values of NDVI and $NDVI_{705}$ (average value of NDVI equal to 0.534, average value of $NDVI_{705}$ equal to 0.392) compared to tree samples of the location 2 (average value of NDVI equal to 0.442, average value of $NDVI_{705}$ equal to 0.259), indicating a better state of health of the vegetation in location 1 compared to location 2.

6. Conclusions

The system developed has several unique and qualifying characteristics: a lower cost compared to other systems available on the market; high spectral resolution; high spatial and temporal resolution and portability. The system is suitable for monitoring a range of small to large areas. The bandwidth is on the order of 10 nm, and the spatial resolution ranges up to the order of millimeters at the scale it was employed in the field survey, allowing a great extent of detail in extracted information.

The comparison of reflectance spectra and indices demonstrates the possibility to obtain accurate estimates of plant ecophysiological state.

Acknowledgements

This work was partially funded by Regione Lazio with the Integrated project for monitoring, requalification and environmental recovery of the Sacco River Valley. The authors would like to acknowledge Marco Marchetti, Luca Shindler, Valerio Della Pelle, Valerio Sassù, Matteo Zappulla for their valuable help during data acquisition.

References

[1] Blackburn GA. Spectral indices for estimating photosynthetic pigment concentrations: a test using senescent tree leaves. *International Journal of Remote Sensing* 1998;**19**:657-675.

[2] Sims AD, Gamon JA. Relationships between leaf pigment content and spectral reflectance across a wide range of species, leaf structures and developmental stages. *Remote Sensing of Environment* 2002;**81**:337- 354. (a)

[3] Sims AD, Gamon JA. Estimation of vegetation water content and photosynthetic tissue area from spectral reflectance: a comparison of indices based on liquid water and chlorophyll absorption features. *Remote Sensing of Environment* 2002;**84**:526-537. (b)

[4] Baret F, Fourty T. Estimation of leaf water content and specific leaf weight from reflectance and transmittance measurements. *Agronomie* 1998;**17**:455-464.

[5] Carter GA, Miller RL. Early detection of plant stress by digital imaging within narrow stress-sensitive wavebands. *Remote sensing of environment* 1994;**50**:295-302.

[6] Gamon JA, Surfus JS. Assessing leaf pigment content and activity with a reflectometer. *New Phytol* 1999;**143**:105-117.

[7] Thenkabail PS, Smith RB, De Pauw E Evaluation of Narrowband and Broadband Vegetation Indices for Determining Optimal Hyperspectral Wavebands for Agricultural Crop Characterization. *Photogrammetric Engineering and Remote Sensing* 2002;**68**(**6**):607-621.

[8] Borengasser M, Hungate WS, Russel W. H. *Hyperspectral Remote Sensing, Principles and Applications. CRC Press;* 2007.

[9] Malthus TJ, Dekker AG. First derivative indices for the remote sensing of inland water quality using high spectral resolution reflectance. *Environment International, Photogrammetric Engineering & Remote Sensing* 1994;**49:**219-229.

[10] Silvestri S, Marani M, Marani A. Hyperspectral remote sensing of salt marsh vegetation, morphology, and soil topography. *Physics and Chemistry of the Earth* 2003;**28**:15-25.

[11] Cenedese A, Miozzi M, Benetazzo A, Paglialunga A, Daquino C, Mussapi R. Vegetation cover analysis using a low budget hyperspectral proximal sensing system. *Annals of Geophysics* 2006;**49**:201-208
[12] Moroni M, Dacquino C, Cenedese A. Mosaicing of hyperspectral images: the application of a spectrograph imaging device. *Sensors* 2012;**12**:10228-10247.
[13] Lillesand TM, Johnson WL, Deuell RL, Lindstrom OM, Eisner DE. Use of Landsat data to predict the trophic state of Minnesota lakes. *Photogrammetric Engineering and Remote Sensing* 1983;**49:**219-229.
[14] Moroni M., Lupo E., Marra E., Cenedese A. (2013). Hyperspectral proximal sensing monitoring of Salix trees in the Sacco river valley (Latium, Italy). In preparation.